

### **GAS Journal of Engineering and Technology (GASJET)**

Volume 2 | Issue 10, 2025

Homepage: <a href="https://gaspublishers.com/gasjet-home/">https://gaspublishers.com/gasjet-home/</a>



ISSN: 3048-5800

## A Method to Determine Design Parameters of the Float in a Rotameter that Satisfies the Measurement Range in a Fixed Cone

Chol-Hwan O, Wi-Song Myong & Kum-Song Ri

Faculty of Mechanical Science and Technology, Kim Chaek University of Technology, Pyongyang 950003, Democratic People's Republic of Korea

Received: 30.08.2025 | Accepted: 03.10.2025 | Published: 22.10.2025

\*Corresponding Author: Kum-Song Ri

**DOI:** 10.5281/zenodo.17418188

Abstract Original Research Article

The rotameter has a relatively low measurement accuracy compared to other flowmeters due to the nonlinearity between the flow rate and the floater position, viscosity difference between the standard and the measuring medium, and the oscillation characteristics of the floater. To improve the measurement accuracy, the taper can be reduced to decrease the nonlinearity, the difference in viscosity can be considered, and the cone length can be made longer to increase the resolution. In practice, however, the installation of the flowmeter may be limited and certain measurement ranges may have to be satisfied.

In this paper, a method is presented to determine the shape and structural parameters of the floater to minimize the oscillation of the floater while satisfying the measurement range when the length of the cone is limited during the installation of the rotameter.

Three-dimensional steady flow simulations were performed to scale where the gravity and the drag force are equal, and then three-dimensional unsteady flow simulations were carried out to analyze the trend of hydrodynamic oscillation force acting on the floater. CFD simulation results showed that the DFC floater was the least oscillatory one in the measurement range. They also showed that four structural dimensions of the DFC floater have a significant influence on the oscillation characteristics.

**Keywords:** rotameter, floater, measurement accuracy, oscillation, verification.

Copyright © 2025 The Author(s). This is an open-access article distributed under the terms of the Creative Commons Attribution-NonCommercial 4.0 International License (CC BY-NC 4.0).

#### 1. Introduction

The flow measurement is very important in the industrial process as well as the measurement of temperature, pressure and level.

The rotameter has a simple structure, a low cost and a convenience of measurement method and use. Rotameters are variable area flowmeters used for the flow measurement of various clean liquids or gases, such as acid liquid, basic liquid, as well as pure water, and are used in many industrial fields.

Rotameters are mounted perpendicular to the horizontal pipeline to measure the flow rate by reading the location of floaters, and the absence of floater oscillation in the measurement is of importance to improve the measurement accuracy.

The conical tube of the rotameter can be made of metal or plastic. In the case of plastic tube, the mold design and fabrication are required, therefore, the design of conical tubes and floaters is very important.

The first consideration in the study of the rotameter is the nonlinearity between the flow rate and the position of the floater, especially, the smaller the length of the conical tube, the larger the nonlinearity appears.

E. Kehat [1] described a constant cross-section, variable area flowmeter. It consists of a rotameter type float fitting closely inside a slitted tube. For a properly designed flowmeter the calibration curve is linear over a wide range of flow rates. Discharge coefficients through the slits and past the float were determined for water and air from calibration curves



of tubes.

The second consideration in the study of the rotameter is the influence of fluid viscosity and the floater shape on the accuracy of the flow measurement.

When measuring the flow rate using a rotameter, the error increases if the viscosity of the fluid to be measured is changed. The actual flow rate becomes smaller than the theoretical flow rate when the viscosity increases, while the actual flow rate becomes larger when the viscosity decreases.

Wei-Jiang et al. [2] investigated the fluid viscosity effects on the orifice rotameter using experimental and theoretical models. Wall jet and concentric annulus laminar theories were adapted to study the influence of viscosity. And a new formula is obtained for calculating the flow rate of viscous fluid. The experimental data were analyzed and compared with the calculated results. At high viscosity the maximum theoretical results error is 6.3 %, indicating that the proposed measurement model has very good applicability.

Dijstelbergen reported and proposed an equation of motion for the float of a rotameter [3]. A sinusoidal pulsation is assumed in order to implement its possible effects on the reading. The calculated mean flow rates are compared with measurements. Float dimensions are said to have a reduction on the error amount of indicated mean flow. The float instability, especially for gases, are also investigated by means of theoretical and experimental means. Author emphasized the importance on defining dynamic behavior of the floats. The author focused to the flow passage narrowing due to the flow jet passing through the float in order to derive an equation of motion. By the pulsating flow, inertia of the float also has an effect on the operation. A motor was utilized in order to produce sinusoidal pulsations, while water in a tank flows due to potential energy. By means of a light beam and a phototransistor, it could be possible to detect the instability of the float.

Guido Belforte et al. [5] proposed the design and the realization of a test bench for flow rate measurement. Various experimental results were presented.

G.S. Harrison [6] investigated the dynamic characteristics of a rotameter experimentally by making frequency response measurements using floats of various shapes and materials in two different liquids. The experimental results are compared with calculations based on a simplified theory which is derived.

With the rapid development of the computer performance, many research institutes have adopted CFD-based design methods to accelerate the production process and improve the product performance, thus reducing the cost of the product development phase.

The physicist Karman, who has been experimenting with flow separation for nearly 30 years, has demonstrated that the vortex phenomena behind the body occur periodically in a range of Reynolds numbers. He defined this condition as the stability condition for the vortex street and proved mathematically.

Grzegorz Pankanin [7] and Jinwen Yang et al. [8] carried out flow simulations around a body in a flow field to describe the Karman vortex behind the body in a certain Reynolds number range and the Karman vortex street depends on the shape of the body.

Jinwen Yang et al. [9] demonstrated that a ringshaped Karman vortex generator installed upstream can eliminate the flow separation phenomenon occurring in the conical diffuser using flow simulation.

Buckle et al. [10] were among the first to use CFD to simulate fluid flow in rotameters. They examined the fluid flow in the rotameter tube under three different fluid regimes: laminar, transient, and turbulent flow. To validate their simulation results, they compared them with velocity contours obtained using laser Doppler anemometry(LDA) [11]. Their study showed that CFD could be a powerful tool for simulating rotameters.

In a subsequent study by Buckle et al. [12], the rotation of the floater and its effects on fluid flow in the rotameter tube was investigated. The authors concluded that the rotation of the floater has a negligible effect on the fluid flow and may not need

to be considered in simulations.

In another study, Kumar et al. [13] simulated a rotameter at various volumetric flow rates and compared the results with experimental data. They demonstrated that CFD and experimental results were in good agreement, with an error of less than 2%. The authors also found that the k- $\omega$  SST turbulence model was the most accurate for simulating fluid flow in the rotameter tube. This model uses a combining function to use k- $\varepsilon$  in lower shear rate zones and standard k- $\omega$  in near-wall regions to obtain more accurate predictions of the fluid flow.

Canli et al. [14] conducted a study to simulate a rotameter with a spherical floater. They compared various mesh sizes and plotted y+ near the tube wall. The authors also compared different turbulence models, such as Reynolds-averaged Navier—Stokes (RANS) and Large Eddy Simulation (LES) models, and examined their effects on the drag force on the floater.

Dara et al. [15] discussed comprehensively on simulation of transient behavior of a rotameter using Computational Fluid Dynamics (CFD) technique. Various methods of dynamic meshing and the reasons behind choosing the diffusion-based model have been discussed. The CFD solver configuration and simulation steps presented in this paper can be used to optimize rotameter designs and improve their performance. Additionally, the simulation results can provide valuable insights into the behavior of the rotameter, allowing designers to identify the

potential areas for improvement and optimization of the design, accordingly. This method is a CFD-based analysis approach close to practice, but the simulation is a labor-consuming work.

As above, there have been many studies on improving the measurement accuracy of rotameters, but there is no published literature on the design method to ensure the measurement accuracy while satisfying the required measurement range in a limited installation space.

Based on the CFD technique, this paper proposes a floater design method to minimize the oscillation of the floater while satisfying the measurement range for a fixed cone length of the rotameter.

#### 2. Methodology

#### 2.1 The measurement principle

When the fluid flows upward in the cone, the floater in the cone will float due to the pressure difference between the top and bottom of the floater. The floater is subjected to a hydrodynamic force due to the gravity, buoyancy and pressure difference of the floater, and when these three forces are drawn, the floater is stopped.

In other words, there exists a flow rate at which the floater stops, and as the flow rate increases, it rises higher and stops in the cone, hence the flow rate can be measured.

According to Mateusz Turkowski et al. [4], the formula for the instantaneous flow rate measurement of the rotameter is

$$Q_{V} \approx \alpha \pi D_{0} h \tan \phi \sqrt{\frac{2gV_{f}(\rho_{f} - \rho)}{S_{f} \rho}}$$
 (1)

Where  $\alpha$  is the flow rate coefficient;  $D_0$  is the minimum diameter of the cone;  $\varphi$  is the half angle of the cone;  $V_f$  is the volume of the floater;  $S_f$  is the maximum cross-area;  $\rho$  is the density of the measuring fluid;  $\rho_f$  is the density of the floater; g is the gravity.

From Eq. (1), the measurement range of the flowmeter depends on the conicity of the cone, the shape and dimensions of the floater and the density of the floater. In addition, the flow rate coefficient of the rotameter depends on the shape and mass of the floater. It is impossible to calculate this coefficient

theoretically so it is obtained by experiments.

# 2.2 Geometric modeling and meshing for CFD simulation

When the rotameter has a small taper and a long taper, it can ensure linearity in the range, widening the measurement range. In reality, however, due to the limitations of the installation space, the length of the cone cannot become longer. Also, nonlinearity is appeared clearly when providing the required measurement range. That is, the measurement accuracy is degraded.

When measuring the flow rate using a rotameter, the floater is subjected to the force due to the vortex behind the floater, in addition to the flow pulsations in the inlet flow. The magnitude of this force depends on the flow conditions, such as the shape of the floater and the shape of the cone, and the larger this force, the more the floater oscillates, which greatly affects the stability of the flow measurement. Therefore, to improve the measurement accuracy of the rotameter, the factors affecting the oscillation of the floater should be found out and minimized.

In this paper, simulation analysis on several floater shapes suitable for the measurement range has performed to determine the floater shape with the minimum amplitude of the force on the floater.

From the geometric conditions required by the process, the internal structural dimensions of the cone can be determined as follows.

**Table 1.** The internal structural dimensions of the cone

Dimensions	Cone length mm	Top diameter mm	Bottom diameter mm	Cone angle
Value	164	29.5	18	4

The floater was preliminarily calculated based on the classical design method and the maximum diameter was 18 mm and the mass was 15 g.

Based on the results, geometric modeling and meshing for CFD simulation was carried out. The meshing was carried out using about 750,000 non-structured tetrahedral elements. The inlet boundary condition was selected as "velocity\_inlet", while the outlet boundary condition was selected as "outflow". And "wall" was selected for the internal cone wall

and the floater surfaces.

#### 2.3 Governing equations and the flow simulation

The governing equations for the flow simulation were selected as the fluid continuity equation and the equation of motion for turbulence, and the "RNG k- $\epsilon$ " model was chosen as the turbulence model.

The fluid continuity equation is

$$\frac{\partial \rho}{\partial t} + \nabla \cdot (\rho \vec{v}) = S_m \tag{2}$$

The equation of motion is

$$\frac{\partial}{\partial t} \left( \vec{\rho v} \right) + \nabla \cdot \left( \vec{\rho v v} \right) = -\nabla p + \nabla \cdot \left( \vec{\tau} \right) + \vec{\rho g} + \vec{F}$$
(3)

Where p is the static pressure,  $\tau$  is the stress tensor,  $\rho g$  and F is the mass force and external force, respectively.



The stress tensor,  $\tau$  is

$$= \tau = \mu \left[ \left( \nabla \vec{v} + \nabla \vec{v} \right) - \frac{2}{3} \nabla \cdot \vec{v} I \right]$$
 (4)

Where  $\mu$  is the molecular viscosity, I is the unit tensor and the  $2^{nd}$  term in the right side indicates the volumetric expansion effect.

"RNG k- $\varepsilon$ " model is

$$\frac{\partial}{\partial t}(\rho k) + \frac{\partial}{\partial x_{i}}(\rho k u_{i}) = \frac{\partial}{\partial x_{j}}(\alpha_{k} \mu_{eff} \frac{\partial k}{\partial x_{j}}) + G_{k} + G_{k} - \rho \varepsilon - Y_{M} + S_{k}$$
(5)

$$\frac{\partial}{\partial t}(\rho\varepsilon) + \frac{\partial}{\partial x_{i}}(\rho\varepsilon u_{i}) = \frac{\partial}{\partial x_{i}}(\alpha_{\varepsilon}\mu_{eff}\frac{\partial\varepsilon}{\partial x_{i}}) + C_{1\varepsilon}\frac{\varepsilon}{k}(G_{k} + C_{3\varepsilon}G_{b}) - C_{2\varepsilon}\rho\frac{\varepsilon^{2}}{k} - R_{\varepsilon} + S_{\varepsilon}$$
 (6)

where  $G_k$  indicates the generation of the turbulent energy due to the average velocity gradients;  $G_b$  indicates the generation due to the buoyancy;  $Y_m$  indicates the contribution of the pulsating expansion in the compressible turbulence to the total dissipation rate;  $\alpha_k$ ,  $\alpha_\varepsilon$  is the reciprocal of the valid Prandtl number of k and  $\varepsilon$ ;  $R_\varepsilon$  is the correction of the dissipation rate  $\varepsilon$ ;  $C_{\varepsilon l}$ ,  $C_{\varepsilon 2}$ ,  $C_{\varepsilon 3}$  are constant as follows.

$$C_{\varepsilon l}$$
=1.42,  $C_{\varepsilon 2}$ =1.68,  $C_{\varepsilon 3}$ =0.09

The numerical simulation was carried out using *Ansys Fluent* 19.2.

The solver was selected as "Pressure-Based Solver" which is commonly used for the numerical simulation of flow fields of low-velocity incompressible fluids, the discretization scheme of the continuity equation was selected as the quadratic upwind scheme, the discretization scheme of the equation of motion was selected as the quadratic scheme, and the pressure-velocity coupling scheme was selected as a "SIMPLE" scheme.

All control variables were set as default values provided by *Fluent*.

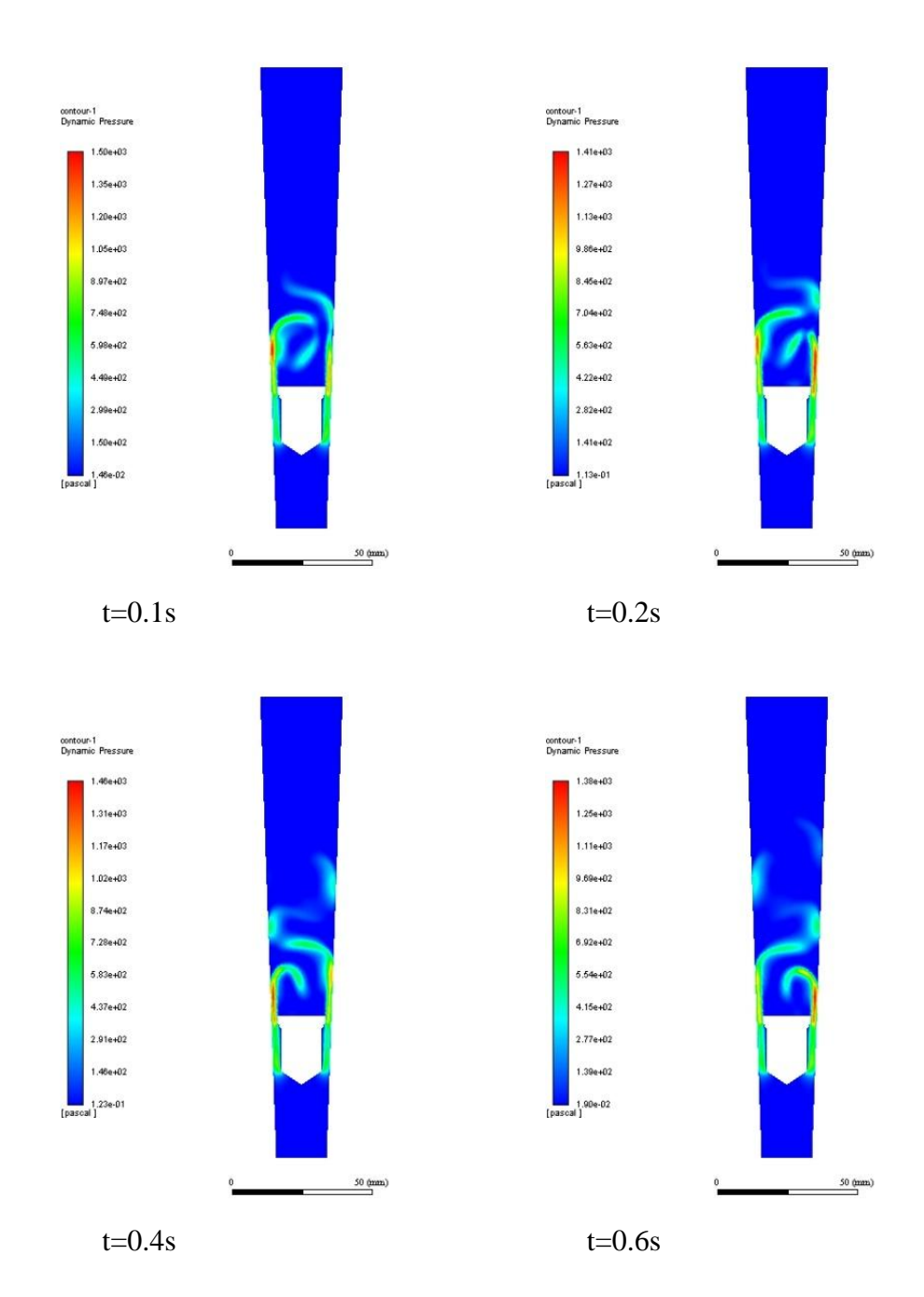
First, a steady flow simulation was carried out to graduate the rotameter.

The graduation was carried out by assuming that the floater is at rest at a certain height and calculating the value of the flow rate when the forces acting on the floater are drawn.

Secondly, to consider the hydrodynamic periodic force acting on the floater, in steady flow calculations, the error bounds of all error terms were converged to 10<sup>-5</sup>. And then the time step was set to 0.001 s and the unsteady flow calculation was carried out.

Fig. 1 shows the flow characteristics around the initially designed floater.

As can be seen, periodic vortices such as the Karman vortex occur above the floater, and hence the floater oscillates during the measurements due to the periodic hydrodynamic forces.



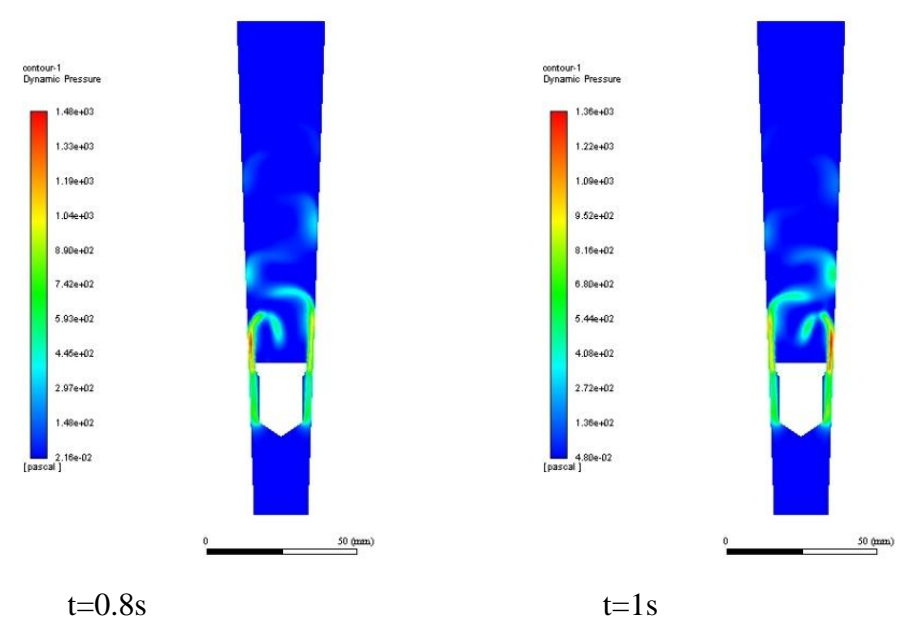


**Fig. 1.** Flow around the floater (Q=0.6m<sup>3</sup>/h).

The maximum amplitudes of hydrodynamic periodic force according to the floater height are listed in Table 2.

Height (mm)	35	65	91	112	132
Flow rate (m <sup>3</sup> /h)	0.4	0.8	1.2	1.6	2
Amplitude (N)	0.056	0.064	0.059	0.055	0.049
Frequency (Hz)	6.7	7.1	7.25	7.38	7.46

**Table 2.** The hydrodynamic periodic force

As can be seen, as the flow rate increases, the magnitude of the periodic hydrodynamic force acting on the floater increases and then decreases.

In order to improve the measurement stability of the floater, the floater must not oscillate during the measurement. Therefore, it is important to minimize this periodic hydrodynamic force when selecting and designing floaters.

#### 3. Simulation results and analysis

In this paper, three types of floaters suitable

for the measurement range are selected and the type with the minimum hydrodynamic oscillation force acting on the floater by numerical simulations is to be selected. And the structural dimensions of the floater with minimum hydrodynamic oscillation force are determined in the selected floater geometry.

From the calculation results, it can be seen that the oscillation of the floater is more apparent at low flow rates. But the degree depends on the shape of floater.

Table 3 shows the magnitude of the hydrodynamic oscillation force acting on the floater.

Table 3. Forces acting on the floater

Flow rate	bullet	DFC	CFH
0.6m <sup>3</sup> /h	0.075	0.056	0.079
1.8m <sup>3</sup> /h	0.038	0.031	0.033

As can be seen in Table 3, DFC floater has the minimum amplitude. Therefore DFC floater is selected and the reasonable dimensions are to be determined.

For the DFC floater, in the case of a flow rate of 0.6m<sup>3</sup>/h, the reasonable dimensions of the floater

with the minimum oscillating force acting on the floater are determined considering the changes of the 5 major dimensions.

The major dimensions of the designed floater are as follows.

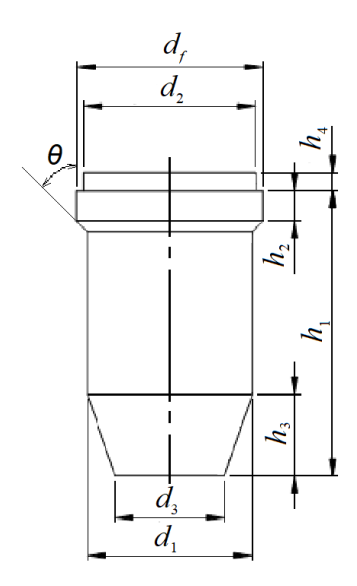


Fig. 2. Structural dimensions of DFC floater

The results of analyzing the amplitude variation of forces acting on the floater for each factor are as follows.

**Table 4.** Amplitude variation of the axial force with variation of  $d_f(q=0.6\text{m}^3/\text{h})$ 

$d_f(mm)$	18	17	16	15
Amplitude(N)	0.0064	0.0072	0.0093	0.0117

As  $d_f$  increases, the stability of the rotameter improves. However, in principle, the upper limit of measurement decreases because the annular cross-section decreases as  $d_f$  increases.

**Table 5.** Amplitude variation of the axial force with variation of  $d_1(q=0.6\text{m}^3/\text{h})$ 

$d_1(mm)$	16	15	14	13
Amplitude(N)	0.0087	0.0085	0.0086	0.0087

The oscillation variation of the floater with the change of  $d_1$  is very faint. This is because  $d_1$  does not have a significant effect on the flow behind the floater.

**Table 6.** Amplitude variation of the axial force with variation of  $d_2(q=0.6\text{m}^3/\text{h})$ 

$d_2(mm)$	16	15.5	15	14.5
Amplitude(N)	0.0083	0.0079	0.0083	0.0096

As  $d_2$  increases, the stability improves, but too much increases cause the vortex behind the floater, thereby the floater oscillation becomes fierce.

**Table 7.** Amplitude variation of the axial force with variation of  $d_3(q=0.6\text{m}^3/\text{h})$ 

<i>d</i> <sub>3</sub> ( <i>mm</i> )	11.5	11	10.5	10
Amplitude(N)	0.0081	0.0079	0.0078	0.0078

**Table 8.** Amplitude variation of the axial force with variation of  $h_I(q=0.6\text{m}^3/\text{h})$ 

$h_1(mm)$	25	26	27	28
Amplitude(N)	0.0098	0.0084	0.0078	0.0077

It can be seen that the fluid flow is somewhat stabilized as  $h_I$  increases. However, the length of the floater should be limited because the minimum annular cross-section could be formed below the floater when increasing  $h_I$ .

**Table 9.** Amplitude variation of the axial force with variation of  $h_2(q=0.6\text{m}^3/\text{h})$ 

$h_2(mm)$	2	2.5	3	3.5
Amplitude(N)	0.0077	0.0079	0.0078	0.0076

**Table 10.** Amplitude variation of the axial force with variation of  $h_3(q=0.6\text{m}^3/\text{h})$ 



<i>h</i> <sub>3</sub> ( <i>mm</i> )	3	4	5	6
Amplitude(N)	0.0076	0.0073	0.0075	0.0072

**Table 11.** Amplitude variation of the axial force with variation of  $h_4(q=0.6\text{m}^3/\text{h})$ 

$h_4(mm)$	0.5	1	2	3
Amplitude(N)	0.0106	0.0099	0.0095	0.0098

If  $h_4$  is too large or very small, the conditions for vortex to appear behind the floater are better. When  $h_4$  has a reasonable value, the cascade behind the floater is close to the streamline, resulting in less vorticity.

**Table 12.** Amplitude variation of the axial force with variation of  $\theta(q=0.6\text{m}^3/\text{h})$ 

$ heta(\degree)$	40	42	44	46
Amplitude(N)	0.0091	0.0085	0.0081	0.0088

Increasing  $\theta$  will change the stability. If  $\theta$  is too large or too small, the oscillation characteristics of the force acting on the floater will be enhanced. Therefore,  $\theta$  needs to be in the range of 40-45° and the best stability is generally obtained with a value of 45°.

Increasing  $\theta$  can increase the upper limit of

measurement of rotameter. Therefore,  $\theta$  is fixed to 45° in this paper.

As can be seen, the parameters that greatly affect the force acting on the floater are  $d_f$ ,  $d_2$ ,  $h_1$ ,  $h_4$ . For these four parameters, the dimensions determined to minimize the oscillation characteristics of the floater are given in Table 13.

**Table 13.** The major dimensions

Dimension	$d_f$	$d_2$	$h_1$	$h_4$	θ(ο)
Value	17	15.5	28	2	45

#### 4. Experiments

Based on the above calculation results, a new rotameter was manufactured, calibrated and verified.



Fig. 3. Newly manufactured rotameter

(a) Optimized floater (b) rotameter

The verification diagram is shown in Fig. 4.

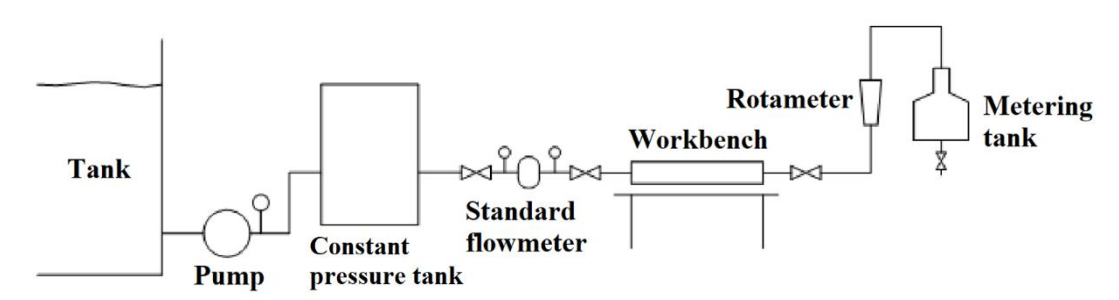


Fig. 4. Verification diagram of the rotameter

During verification experiments, the flow rate was changed by adjusting the gate valve behind the constant pressure tank and the flow rate was set by the scale of the floater flowmeter. The average flow rate was calculated by measuring the time taken to fill the metering tank (volume:  $50 \pm 10$ -3 L) with a

stopwatch (accuracy:  $\pm 0.1$  s).

The results of three measurements at the same flow rate point by adjusting the gate valve to increase the flow rate and then decrease again are as follows.

**Table 14.** The verification experiment results

	Flow rate		Time, s				Standard flow rate, m <sup>3</sup> /h				Error
No	in rotameter	Unit	1	2	3	평균 값	1	2	3	평균값	(%)



1	0.4	m <sup>3</sup> /h	461.5	450	461.5	457.7	0.39	0.40	0.39	0.39	-2.5
2	1.0	m <sup>3</sup> /h	183.5	182	185.5	183.7	0.98	0.99	0.97	0.98	-2.0
3	1.4	m <sup>3</sup> /h	129.5	130.5	131.4	130.5	1.39	1.38	1.37	1.38	-1.4
4	2.0	m <sup>3</sup> /h	87	87.5	87.8	87.4	2.07	2.06	2.05	2.06	3.0

As can be seen from the results, the newly designed and manufactured rotameter has no more than 3% measurement error.

#### 5. Conclusion

In this paper, a method is presented to determine the shape and structural parameters of the floater to minimize the oscillation of the floater while satisfying the measurement range when the length of the cone is fixed.

The simulation results showed that the DFC floater was the least oscillating floater in a given cone and measurement range. It also showed that four structural dimensions of the DFC floater have a significant influence on the oscillation characteristics.

The designed floater was manufactured and introduced into the process pipeline with a measuring range of 0.6~2m<sup>3</sup>/h and no oscillation of the floater was observed during the measurement.

Therefore, the method presented here is considered to be an effective method to improve the measurement accuracy while satisfying the installation conditions and measurement range.

#### Acknowledgment

I would like to take the opportunity to express my hearted gratitude to all those who make a contribution to the completion of my article.

#### Conflict of interest

The authors declare that there is no conflict of interest regarding the publication of this paper.

#### **Disclosure statement**

No potential conflict of interest was reported by the authors.

#### **Data Availability**

The data that support the findings of this study are available within the article.

#### **REFERENCES**

- 1. E. Kehat, 1964. Constant cross-section, variable area flowmeter, *Chemical Engineering Science*, 1965, vol. 20, 425-429
- 2. Wei-Jiang et al., 2016. The effects of fluid viscosity on the orifice rotameter, *Measurement science review*, 16, (2016), No. 2, 87-95
- 3. Dijistenlbergen H.H., 1964. Rotameter Dynamics, *Chemical Engineering Science*, 19, 853–865.
- 4. Mateusz Turkowski, Artur Szczecki, Maciej Szudarek, 2019, Minimization of the Settling Time of Variable Area Flowmeters, *Sensors*, 19
- 5. Massimiliana Carello etc, 1997. Test bench for flow rate Measurement: Calibration of Variable Area Meters, *Measurement*, 20 (1), 67–74.
- 6. Harrison G.S., Armstrong W.D., 1960. The Frequency response of Rotameters, *Chemical Engineering Science*, 12, 253–259.
- 7. Grzegorz Pankanin, 2019. Simulation of Influence of Mechanical Elements on Karman Vortex Street Parameters, *INTL Journal of Electronics and Telecommunications*, 65 (2), 229-234
- 8. Jinwen Yang, Yufei Zhang, Haixin Chen, Song Fu, 2020. Unsteady flow control of a plane diffuser based on a Karman-vortex generator, *AIP Advances*, 10
- 9. Jinwen Yang, Yufei Zhang, Haixin Chen, Song F, 2020, Flow separation control in a conical diffuser with a Karman-vortex generator, *Aerospace*



Science and Technology, 106

- 10. U. Bückle, F. Durst, H. Köchner, A. Melling, Investigation of a floating element flowmeter, Flow Meas. Instrum. 3 (4) (1992) 215–225
- 11. F. Durst, A. Melling, J.H. Whitelaw, Principles and Practice of Laser-Doppler Anemometry, Vol. 76, NASA STI/Recon Technical Report A, 1976
- 12. U. Bückle, F. Durst, H. Köchner, A. Melling, Further investigation of a floating element flowmeter, Flow Meas. Instrum. 6 (1) (1995) 75–78
- 13. P. Kumar, V. Seshadri, Analysis of flow

- through rotameter using CFD, Int. J. Emerg. Technol. Adv. Eng. 5 (2015)
- 14. Eyub CANLI, Ali ATES, 2013, Steady and transient flow structure in a rotameter with a ball floater, *EPJ Web of Conferences*, Vol. 213, EDP Sciences, 2019, p. 12
- 15. Dara Rahmat Smaii, Seyed Hassan Hashemabadi, Payam Margan, 2024, CFD based design gas rotameters: Dynamic mesh transient simulation, *Flow Measurement and Instrumentation*, 95